J Fluoresc (2010) 20:1255–1265
DOI 10.1007/s10895-010-0677-2

ORIGINAL PAPER

# Ethynylated Triphenylamine Monoboronic acid Chemosensors: Experimental and Theoretical Studies

**Lina Chi · Yubo Wu · Xin Zhang · Shaomin Ji · Jingyin Shao · Huimin Guo · Xin Wang · Jianzhang Zhao**

Received: 8 March 2010 / Accepted: 5 May 2010 / Published online: 18 May 2010


**Abstract** New ethynylated triphenylamine boronic acid sensors **1** and **2** were designed and the photophysical properties, as well as the binding with tartaric acid and mandelic acid were studied. We found the emission intensity of the sensors is sensitive to the polarity of the solvents and the emission of sensor **2** is sensitive to protic solvents. Theoretical calculations on the low-lying excited states of these sensors predicted d-PET effect. Experimental observations show either a-PET effect or no significant PET effect for the sensors. The sensitivity of the emission of the sensors toward solvent polarity is used to rationalize the observed emission intensity-pH profiles.

**Keywords** Boronic acid · Fluorescent chemosensors · DFT · PET

**Electronic supplementary material** The online version of this article (doi:10.1007/s10895-010-0677-2) contains supplementary material, which is available to authorized users.

L. Chi · Y. Wu · X. Zhang · S. Ji · J. Shao · J. Zhao (✉)
State Key Laboratory of Fine Chemicals,
School of Chemical Engineering,
Dalian University of Technology,
Dalian 116012, People's Republic of China
e-mail: zhaojzh@dlut.edu.cn

H. Guo (✉)
Department of Chemistry, School of Chemical Engineering,
Dalian University of Technology,
Dalian 116012, People's Republic of China
e-mail: guohm@dlut.edu.cn

X. Wang
Faculty of Chemistry, Sichuan University,
Chengdu 610064, People's Republic of China

## Introduction

Among the fluorescent chemosensors, fluorescent boronic acid sensors are unique, due to their covalent binding nature with analytes [1–19], conversely most of the chemosensors for organic analytes are based on hydrogen bondings [20–24]. The binding and sensing of analytes with boronic acid sensors can be accomplished in aqueous media, thus boronic acid sensors paved way for in vivo applications, such as monitoring blood glucose level for patients with diabetes [25–29].

Besides the unique covalent binding motif of boronic acid chemosensors, the photophysical properties of the fluorophores as well as the fluorescence transduction mechanism have to be considered for a successful sensor design [1–3, 30]. The most popular fluorophores for boronic acid sensors are anthracene [31–34], naphthalimide [10, 35, 36], naphthalene [37, 38], etc. Furthermore, sensing mechanisms of photo-induced electron transfer (PET, usually the fluorophore as the electron acceptor of the PET process, thus a-PET is used to describe these sensors) and intramolecular charge transfer (ICT) have been extensively used in fluorescent boronic acid sensors [38]. However, the existing fluorophores of boronic acid sensors suffer from short excitation/emission wavelength, small Stokes shifts, etc [31, 32]. The a-PET mechanism gives poor fluorescence transduction efficiency at acidic pH (the intrinsic drawbacks of a-PET sensors) [30]. The diversity of the fluorophores as well as the sensing mechanisms of the boronic acid sensors needs to be explored to improve the molecular sensing performance of the sensors.

Recently we have embarked on synthesis of boronic acid sensors [32–34, 39–43]. We found that d-PET sensors (fluorophore as the electron donor of the PET) can be developed with the carbazole fluorophore, which show reduced background fluorescence emission at acidic pH [42, 43]. Thus, enhanced fluorescence transduction efficiency at acidic pH was observed in the presence of analytes, such as tartaric acid [42, 43]. Normal a-PET sensors give poor response in this acidic pH range, due to the strong background emission, caused by the protonation of the nitrogen atom in the sensor [30, 32, 44]. We envisioned that with electron-donating fluorophores, such as triphenylamines, new d-PET sensors can be designed and recognition of tartaric acid can be realized in acidic pH range, with which the binding is much stronger than that at neutral or basic pH ranges.

DFT/TDDFT calculations have been successfully used for study of fluorophores [42, 43, 45–49]. However, very few DFT/TDDFT calculations were used for rational design of fluorescent chemosensors and study of the photophysical properties of fluorescent chemosensors. We have applied DFT/TDDFT calculations in the rational design of the fluorescent chemosensors and some promising results have been obtained [42, 43, 45]. For example, the d-PET effect of carbazole based boronic acid sensors has been rationalized with DFT/TDDFT calculations [42, 43]. Furthermore, OFF-ON fluorescence thiol probes were successfully designed with the guide of DFT/TDDFT calculations [45].

Herein we designed new boronic acid sensors **1** and **2** based on ethynylated triphenylamines (TPA) (Scheme 1), which is known as a strong electron donor. Large π-conjugation frameworks were established by incorporating ethynyl phenyl groups in the molecules with Sonogashira cross coupling reactions (Scheme 1). We found the ICT effect imposes drastic influence on the photophysical properties of the sensors, such as the excitation/emission wavelength, the Stokes shifts and the sensitivity of emission to polarity of the solvents and to protic solvents. DFT/TDDFT calculations predicted d-PET effect for sensors **1** and **2**, i.e. the emission is predicted to be weak at acidic pH but stronger at neutral pH. However, no d-PET effect was observed for these sensors. Instead, normal a-PET effect was observed for sensor **1** and no significant PET effect was observed for sensor **2**. For sensor **2**, a molecule with extra electron donating group of dimethylamino groups, the lack of PET effect is proposed to be due to the elevated energy level of the HOMO of the sensors, which is supposed to be higher than the energy level of the lone electron pair on the nitrogen atom (alkylamine). The structure of the binding complex of sensor **1** was studied with DFT optimization and the optimized zwitterionic structure (methanol-inserted, intramolecular hydrogen bond form) is in agreement with single crystal structure of similar complexes. Thus we demonstrated the promise as well as the limitations of the DFT/TDDFT calculation in the study of the photophysical properties of chemosensors. These systematic investigations on the photophysical properties of the triphenylamine based boronic acid sensors are of great interest for future development of new fluorophores and fluorescent chemosensors, as well as for study of photophysics of fluorophores and chemosensors.

## Experimental

### Materials and general methods

NMR spectra were recorded on a Bruker 400 MHz spectrophotometer ($CDCl_3$ or $CDCl_3/CD_3OD$ as solvents, tetramethylsilane as the standard, TMS, $\delta$=0.00 ppm). Mass spectrometric data were obtained on a HP1100LC/MSD mass spectrometry and a LC/Q-TOF MS spectrometry. Fluorescence spectra were measured on a F4500 fluorospectrometer (Hitachi) or a CRT 970 fluorescence spectrometer. Absorption spectra were recorded on a Perkin-Elmer-Lambda-35 UV/VIS spectrophotometer. Quartz cuvettes were used in all fluorescence studies. A 0.05 M NaCl (52.1% methanol in water, w/w) ionic buffer was used in the experiment. All pH measurements were recorded on a Delta 320 Microprocessor pH meter (Mettler Toledo), which was calibrated using standard buffer solutions. The pH was controlled using minimum volumes of sodium hydroxide and hydrochloric acid solutions. The fluorescence spectra of the sensors in the presence of the analytes were recorded as increasing amounts of the analytes were added to the solution. Titration curves were generated using the Origin 5.0 (Microcal software). For the measuring of the binding constants, the sensor solution was equilibrated over night before measurement. The binding constants were calculated using SigmaPlot 2000 (SPSS Inc.).

### 4-formyl triphenylamine (compound **3**)

To a solution of triphenylamine (5.0 g, 40.8 mmol) in 15 mL dry DMF, $POCl_3$ (3.0 g, 19 mmol) was added dropwise with stirring, and the temperature was kept below 20°C. The reaction mixture was maintained at room temperature for 0.5 h, and then heated at 100°C for 1.5 h. Then the reaction solution was poured into ice water, and the precipitated solid was filtered and washed with water. The crude product was purified by column chromatography (silica gel, dichloromethane as eluent) to afford a yellow solid. 4.6 g. yield: 83.0%. $^1$H NMR (400 MHz, $CDCl_3$ TMS) $\delta$: 9.81 (s, H, CHO), 7.69 (d, 2H, $J$=8.4 Hz, ArH), 7.34 (m, 4H, ArH), 7.18 (m, 6H, ArH), 7.03 (d, 2H, $J$=8.8 Hz, ArH).

**Scheme 1** Synthesis of sensors **1** and **2**

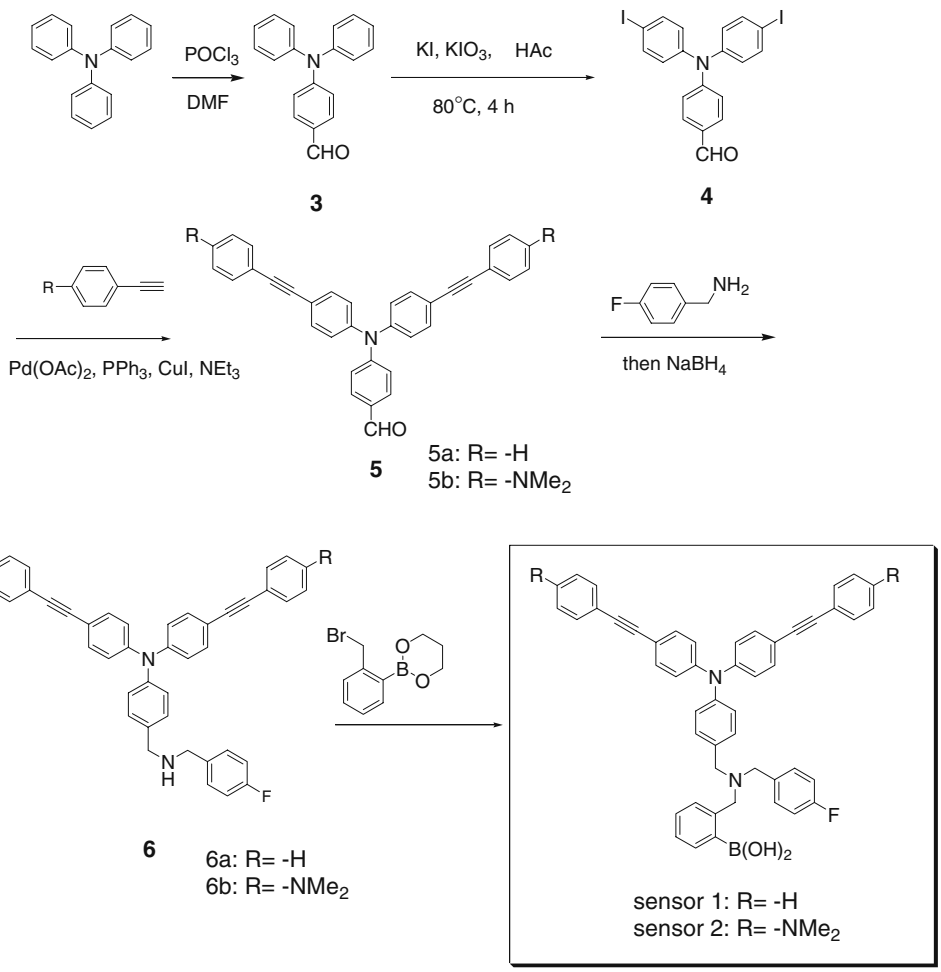


4-(bis(4-iodophenyl)amino)benzaldehyde (compound **4**)

To a solution of 4-formyl triphenylamine (**3**) (4.6 g, 16.8 mmol) and KI (3.91 g, 24.6 mmol) in acetic acid (60 mL) and water (6 mL), potassium iodate (3.84 g, 18.2 mmol) was added and the mixture was stirred and heated at 80°C for 4 h. The solvent was removed under reduced pressure, the black residue was dissolved in ethyl acetate and washed several times with water and sodium bicarbonate solution. The organic phase was dried over anhydrous $Na_2SO_4$, filtered, and evaporated to give the product as a yellow solid. 4.8 g, yield 54.4%. $^1$H NMR (400 MHz, $CDCl_3$ TMS) $\delta$: 9.84 (s, H, CHO), 7.70 (d, 2H, $J$=8.0 Hz, ArH), 7.61 (d, 4H, $J$=7.6 Hz, ArH), 7.04 (d, 2H, $J$=8.0 Hz, ArH), 6.88 (d, 4H, $J$=8.0 Hz, ArH).

4-(bis(4-(2-phenylethynyl)phenyl)amino)benzaldehyde ( compound **5a**)

Under argon atmosphere, to a solution of 4-(bis(4-iodophenyl) amino)benzaldehyde (**4**) (1.19 g, 2.86 mmol) in 16 mL triethylamine, palladium acetate (10.9 mg, 0.05 mmol), triphenylphosphine (15.0 mg, 0.06 mmol), CuI (10.9 mg, 0.06 mmol) and phenylacetylene (700 mg, 6.86 mmol) were added and the resulting mixture was heated at 80°C for 10 h. Then the solvent was removed in vacuum, the black residue was dissolved in $CH_2Cl_2$ and washed several times with water. The organic phase was dried over anhydrous $Na_2SO_4$, filtered, and concentrated. The crude product was purified by column chromatography (silica gel, dichloromethane/ petroleum ether, 1:1, V/V) to afford a green solid, 0.575 g. Yield: 53.5%. $^1$H NMR (400 MHz, $CDCl_3$ TMS) $\delta$: 9.86 (s, H, CHO), 7.75−7.73 (d, 2H, $J$=8.4 Hz, ArH), 7.54−7.48 (m, 8H, ArH), 7.35−7.34 (d, 6H, $J$=4.8 Hz, ArH), 7.14−7.11 (m, 6H, ArH). TOF EI-MS: $m/z$ (positive ion mode): calcd 473.1780, found 473.1788.

*N*-(4-((4-fluorobenzylamino)methyl)phenyl) -4-(2-phenylethynyl)-N-(4-(2-phenylethynyl)phenyl) benzenamine (compound **6a**)

Under argon atmosphere, to a stirred solution of 4-(bis (4-(2-phenylethynyl)phenyl) amino) benzaldehyde (**5a**)

(500 mg, 0.89 mmol) in 27 mL ethanol/THF (3:2, V/V), 4-fluorobenzylamine (132 mg, 1.05 mmol) was added and the resulting mixture was heated at 80°C for 24 h. Then $NaBH_4$ (151 mg, 3.99 mmol) was added. The mixture was stirred at room temperature for an additional 1 h. The solvent was removed under reduced pressure, and the resulting solid was mixed with 20 mL of water and the aqueous phase was extracted with $CH_2Cl_2$ (3×30 mL). Remaining particulate sodium salts were vacuum filtered, and the filtrate was collected and dried over anhydrous $Na_2SO_4$. The solvent was removed under vacuum and the crude product was purified with column chromatography (silica gel, ethyl acetate/ petroleum ether, 5:1, V/V) to afford yellow oil. 290 mg, yield: 47.2%. $^1$HNMR (400 MHz, $CDCl_3$ TMS) $\delta$: 7.51–7.48 (m, 4H, ArH), 7.40–7.38 (d, 4H, $J$=8 Hz, ArH), 7.31–7.28 (m, 8H, ArH), 7.25–6.23 (d, 2H, $J$=8 Hz, ArH), 7.08–7.05 (d, 2H, $J$=8.0 Hz, ArH), 7.03–6.97 (m, 6H, ArH), 3.74–3.73 (m, 4H), 3.78–3.77 (m, 4H). ESI-mass: $m/z$ (positive ion mode): $[M+H]^+$ calcd 583.2, found 583.5.

Sensor **1**

To a stirred solution of (**6a**) (290 mg, 0.61 mmol) in 20 mL acetonitrile, 2-(2-bromomethylphenyl)-1,3,2-dioxaborinane (234 mg, 0.9 mmol) and $K_2CO_3$ (338 mg, 2.4 mmol) were added and the mixture was refluxed at 90°C for 24 h. After the reaction, the solvent was removed in vacuum, and the resulting solid was mixed with 20 mL of water and the aqueous phase was extracted with $CH_2Cl_2$ (3×30 mL). The organic phase was dried over $Na_2SO_4$. The solvent was removed under vacuum and the crude product was purified with column chromatography (silica gel, dichloromethane/ MeOH, 50:1, V/V) to afford a yellow solid 250 mg. Yield: 70.1%. Mp 151.4–153.7°C. $^1$HNMR (400 MHz, $CDCl_3$ TMS) $\delta$: 7.53–7.50 (m, 4H, ArH), 7.42–7.40 (d, 4H, $J$=8 Hz, ArH), 7.36–7.29 (m, 10H, ArH), 7.26–6.23(m, 2H, ArH), 7.21–7.17 (m, 2H, ArH), 7.15–7.13 (m, 2H, $J$=8 Hz, ArH), 7.04–7.01 (m, 2H, ArH), 3.69–3.55 (m, 6H). $^{13}$CNMR (100 MHZ, $CDCl_3$) 161.31, 147.27, 146.33, 140.99, 136.86, 136.50, 133.77, 132.91, 132.00, 131.72, 131.11, 130.62, 130.56, 130.35, 129.84, 128.51, 128.39, 128.24, 127.82, 126.99, 126.30, 125.04, 124.64, 123.99, 123.73, 117.70, 115.69, 115.48, 89.58, 89.29, 62.20, 57.62, 57.52. HR-MS: $m/z$ (positive ion mode): $[M+H]^+$ calcd 717.3071, found 717.3089.

4-(bis(4-(2-(4-(dimethylamino)phenyl)ethynyl) phenyl) amino)benzaldehyde (compound **5b**)

Under argon atmosphere, to a stirred solution of 4-(bis(4-iodophenyl)amino)benzaldehyde (4) (979 mg, 1.96 mmol) in 20 mL triethylamine, palladium acetate (4.16 mg, 0.019 mmol), triphenyl phosphine (9.7 mg, 0.03 mmol), CuI (7.03 mg, 0.037 mmol) and 4-Ethynyl-N,N-dimethylaniline (647 mg, 4.46 mmol) were added and the mixture was heated at 80°C for 10 h. The solvent was removed in vacuum, the black residue was dissolved in $CH_2Cl_2$ and washed several times with water. The organic phase was dried over anhydrous $Na_2SO_4$, filtered, and concentrated. The crude product was purified by column chromatography (silica gel, dichloromethane/ petroleum ether as eluent, 1:1, V/V) to afford a green solid. 520 mg, yield: 49.9%. $^1$HNMR (400 MHz, $CDCl_3$ TMS) $\delta$: 9.84 (s, H, CHO), 7.73–7.71 (d, 2H, $J$=8.0 Hz, ArH), 7.46–7.44 (d, 4H, $J$=8 Hz, ArH), 7.41–7.39 (d, 4H, $J$=8.0 Hz, ArH), 7.10–7.08 (d, 6H, $J$=8.0 Hz, ArH), 6.67–6.65 (d, 4H, $J$=8.0 Hz, ArH), 2.99 (d, 12H, $J$=8.0 Hz). ESI-mass: $m/z$ (positive ion mode): $[M+H]^+$ calcd 560.3, found 560.5.

N-(4-((4-fluorobenzylamino)methyl) phenyl)-4-(2-phenylethynyl)-N-(4-(2-phenyl-ethynyl) phenyl)benzenamine (compound **6b**)

Under argon atmosphere, to a stirred solution of 5b (450.0 mg, 0.82 mmol) in 27 mL ethanol/THF (3:2, V/V), was added 4-fluorobenzylamine (1.0 mmol, 125.0 mg) and the mixture was heated at 80°C for 24 h. Then $NaBH_4$ (4.0 mmol, 69.0 mg) was added. The mixture was stirred for an additional 1 h. The solvent was removed in vacuum, and the resulting solid was mixed with 20 mL of water and the aqueous phase was extracted with $CH_2Cl_2$ (3×30 mL). The organic phase was dried over anhydrous $Na_2SO_4$. The solvent was removed under vacuum and the crude product was purified with column chromatography (silica gel, ethyl acetate/ petroleum ether, 5:1, V/V) to afford yellow oil. 270 mg, yield: 50%. $^1$HNMR (400 MHz, $CDCl_3$ TMS) $\delta$: 7.40–7.32 (m, 8H, ArH), 7.25–7.23 (d, 4H, $J$=8 Hz, ArH), 7.08–7.06 (d, 2H, $J$=8.0 Hz, ArH), 7.02–6.99 (d, 6H, $J$=12.0 Hz, ArH), 6.66–6.64 (d, 4H, $J$=8.0 Hz, ArH), 3.81 (m, 4H), 3.76 (m, 4H), 2.99 (d, 12H, $J$=8.0 Hz). HRMS: $m/z$ (positive ion mode): $[M+H]^+$ calcd 669.3394, found 669.3384.

Sensor **2**

To a stirred solution of (6b) (250.0 mg, 0.39 mmol) in 20 mL acetonitrile, 2-(2-bromomethylphenyl)-1,3,2-dioxaborinane (119 mg, 0.468 mmol)and $K_2CO_3$ (1.56 mmol, 215.28 mg) were added and refluxed at 90°C for 24 h. After the reaction, the solvent was removed in vacuum, and the resulting solid was mixed with 20 mL of water and the aqueous phase was extracted with $CH_2Cl_2$ (3×30 mL). The organic phase was dried over sodium sulfate. The solvent was removed under vacuum and the crude product was purified with column chromatography (silica gel, dichloromethane/ MeOH, 50:1, V/V) to afford a yellow solid

150 mg. Yield: 47.6%. Mp 155.9–157.8°C. $^{1}$HNMR (400 MHz, $CDCl_3$ TMS) $\delta$: 7.40–7.36 (m, 9H, ArH), 7.3–7.28 (d, 4H, $J$=8.0 Hz, ArH), 7.12–7.10 (d, 2H, $J$=8.0 Hz, ArH), 7.03–6.98 (m, 6H, ArH), 3.74 (s, 2H), 3.62 (s, 2H), 3.55 (s, 2H), 2.98 (d, 12H, $J$=8.0 Hz). $^{13}$C NMR: (100 MHz, $CDCl_3$ TMS) 162.11, 150.26, 146.60, 136.84, 132.82, 132,54, 131.73, 131.64, 131.46, 131.03, 130.58, 127.79, 124.63, 123.85, 118.64, 115.66, 115.45, 112.13, 110.67, 90.39, 87.48, 62.13, 57.45, 40.42. HRMS: $m/z$ (positive ion mode): $[M + H]^+$ calcd 803.3933, found 803.3912.

## Theoretical calculations

The ground state structure of sensors **1** and **2** were optimized using density functional theory (DFT) with B3LYP functional and 6-31G (d) basis set. The excited state related calculations were carried out with the time dependent density functional theory (TD-DFT) with the optimized structure of the ground state (DFT/6-31G(d)). There are no imaginary frequencies in frequency analysis of all calculated structures, therefore each calculated structure is a local energy minimum. All these calculations were carried out with Gaussian 03 [50].

## Results and discussions

The design rational of the sensor **1** and **2** lies in the notion that triphenylamine (TPA) is a strong electron donor, which is a prerequisite for the d-PET effect [42, 43, 51]. However, the fluorescence of TPA is weak, therefore π-conjugation is introduced to enhance the emission and extend the emission to longer wavelength. First 4-formyltriphenylamine was prepared with Vilsmeier reaction. Then the aldehyde was iodized [52]. Sonogashira cross coupling reaction was employed to connect the ethynylated phenyl group to TPA moiety. With reductive amination, the amine **6** was obtained (Scheme 1). Finally boronic acid group was introduced. F substitution and *para*-dimethylamino group were used to improve the possible d-PET effect. All the compounds were obtained in satisfying yields (Scheme 1).

The excitation and emission spectra of sensor **1** and sensor **2** were studied (Fig. 1). The excitation and emission maxima of sensor **1** are 392 nm and 474 nm, respectively. Compared to the emission of anthracene, a popular fluorophore used in boronic acid sensor [32], the emission of sensor **1** is red-shifted by ca. 50 nm. For sensor **2**, however, the excitation/emission bands are centered at 390 nm and 412 nm, respectively. The Stokes shift of sensor **1** is 82 nm, vs. sensor **2** with Stokes shift of only 22 nm. Based on these observations, we propose that the

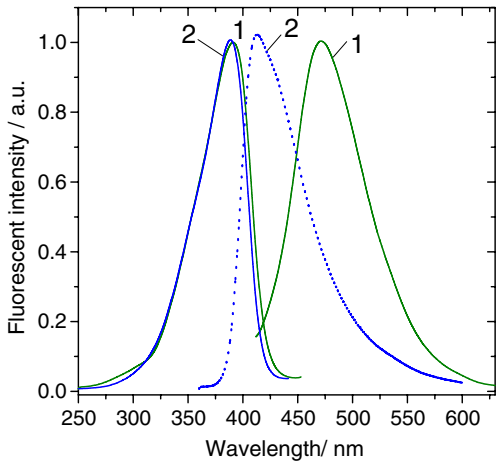


**Fig. 1** Normalized excitation and emission spectra of sensor **1** and sensor **2**. For sensor **1**, λex=392 nm, λem=474 nm. For sensor **2**, λex =390 nm, λem=412 nm. $1.0\times10^{-6}$ mol $dm^{-3}$ of sensors in 0.05 mold $dm^{-3}$ NaCl ionic buffer (52.1% methanol and 4.0% THF in water). pH 7.20, 20°C

ICT feature of sensor **1** is more significant than that of sensor **2**, thus the ethynylated phenyl moiety can be considered as electron deficient group. This is important for future design of fluorophores with ethynylene groups. Longer excitation/emission wavelength and larger Stokes shifts are desired for fluorescent chemosensors, because the background or the auto-fluorescence of bio-sample can be suppressed with longer excitation wavelength, which is beneficial for analytical purpose, especially in vivo fluorescence bioimaging [45].

The emission intensity-pH profile of the sensors without and in the presence of analytes was studied (Fig. 2). For sensor **1**, the emission band centered at 460 nm (at basic pH) and the spectra red-shifted slightly with increasing the pH of the media. This is probably due to the deprotonation of the $Ar_3N$ amine moiety. We demonstrated that ethynyl group is electron-withdrawing [43], protonation of the $Ar_3N$ amine will reduce the ICT feature of the fluorophore, and thus emission appears at relatively shorter wavelength.

Normal a-PET effect was observed, i.e. enhanced fluorescence emission was observed in the acidic pH range but diminished fluorescence emission intensity was observed in the neutral and basic pH range (Fig. 2) [1–3, 30–33, 39–43]. This emission intensity-pH profile is due to the protonation of the nitrogen atom at acidic pH range, thus the a-PET effect is suppressed, as a result the fluorescence emission is enhanced [1–3, 10, 30]. Apparent $pK_a$ values of 4.63±0.06 was determined and this value is in agreement with the similar Wulff type of boronic acid sensors [1–3, 30–33, 39–43].

The emission intensity-pH profile of sensor **1** was also studied in the presence of analytes, such as mandelic acid and tartaric acid (Fig. 2b). The emission of the sensor **1** was

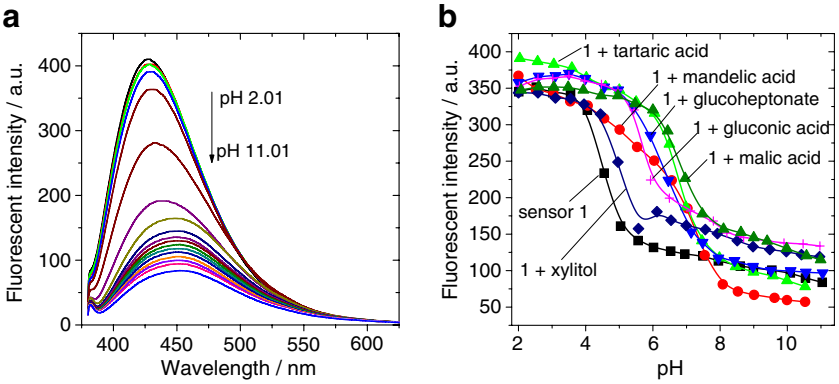


**Fig. 2** Fluorescent intensity-pH profile of sensor **1**. (**a**) the emission spectral changes vs. pH of the solution. (**b**) the pH titration curves of the sensor **1** with and without analytes (0.025 mol $dm^{-3}$). λex= 375 nm. $1\times10^{-6}$ mol $dm^{-3}$ of sensor **1** in 0.05 mol $dm^{-3}$ NaCl ionic buffer (52.1% methanol in water, containing 4% THF). p$K_a$ for the blank sensor and in the presence of analytes. Blank, 4.63±0.06; mandelic acid: 6.79±0.10; tartaric acid: 6.71±0.06; sodium glucoheptonate: 6.38±0.04; xylitol: 5.16±0.11; gluconic acid: 5.88±0.08; malic acid: 6.88±0.05

enhanced at pH 4.0–pH 8.0 in the presence of analytes, and apparent p$K_a$ values of 6.79±0.10 and 6.71±0.06 were observed in the presence of mandelic acid and tartaric acid, respectively. pH 5.5 was selected for the measurement of the binding constant of sensor **1** with mandelic acid and tartaric acid, and $(1.05\pm0.20)\times10^4$ $M^{-1}$ ($r^2$=0.97) and $(5.74\pm1.08)\times10^3$ $M^{-1}$ ($r^2$=0.98) were observed, respectively. Thus the sensor **1** shows good chemoselectivity toward mandelic acid over tartaric acid (Fig. 3).

The emission intensity-pH profile of the sensor **1** in the presence of monosaccharide was also studied but only minor enhancement was observed (see Supplementary data). This poor fluorescence transduction maybe due to weak binding of the sensor with monosaccharides.

The emission spectra of sensor **2** with variation of the pH were also studied and different profile was observed

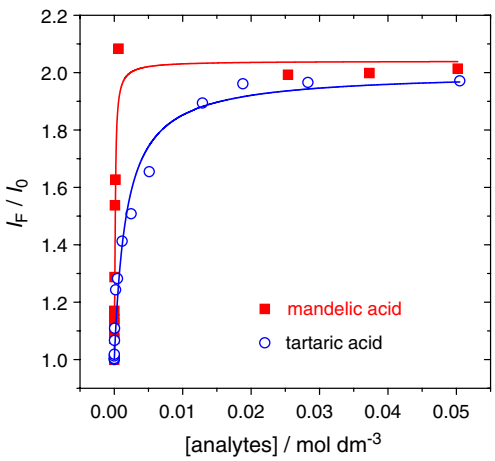


**Fig. 3** Binding curves of sensor **1** with mandelic acid and tartaric acid. $1.0\times10^{-6}$ mol $dm^{-3}$ of sensor **1** in 0.05 mol $dm^{-3}$ NaCl ionic buffer (52.1% methanol in water, containing 4.0% THF). λex= 390 nm, λem=474 nm

(Fig. 4). First, the emission spectra show blue-shift with increasing the pH (from pH 2.0). This blue-shift is in contrast to the property of sensor **1**, which show red-shifted emission band with increasing the pH (Fig. 2). We attribute the blue-shifting of the emission of sensor **2** to the decreased ICT feature of the fluorophore with increasing the pH (thus deprotonation of the dimethylamino group). Second, the fluorescence emission of sensor **2** shows sharp decrease by increasing the pH from pH 2.0 to pH 3.0. Third, the emission intensity of sensor **2** is weak and almost unaffected by variation of the pH in the range of pH 4.0–pH 11.0. The emission intensity-pH profile of the sensor **2** in the presence of analytes was also studied and no significant enhancement was observed. This insensitivity of the emission to pH infers that the a-PET effect of sensor **2** is not significant. The fluorescence enhancement by decreasing the pH is due to the protonation of the nitrogen atom of the dimethylamino group [45, 46, 53]. We attribute the lack of the a-PET effect is probably due to the high energy level of the HOMO energy level of the sensor, caused by the strong electron donating nature of the triphenylamine moiety and the dimethylamino groups (vide infra).

The low emission intensity of sensor **2** in the buffer solution maybe due to the quenching effect of the protic solvents on the emission of the fluorophores [46, 54]. The possible interaction responsible for the quenching of the fluorescence maybe the solute-solvent hydrogen binding (H-bond, the dimethylamino moiety as the H-bond acceptor), which is known to be able to quench the emission of fluorophores [46, 54].

In order to investigate the dependence of the emission of sensors **1** and **2** on the polarity of solvents, the emission spectra of sensor **1** and sensor **2** in selected solvents were studied (Fig. 5). The results show that the emission of

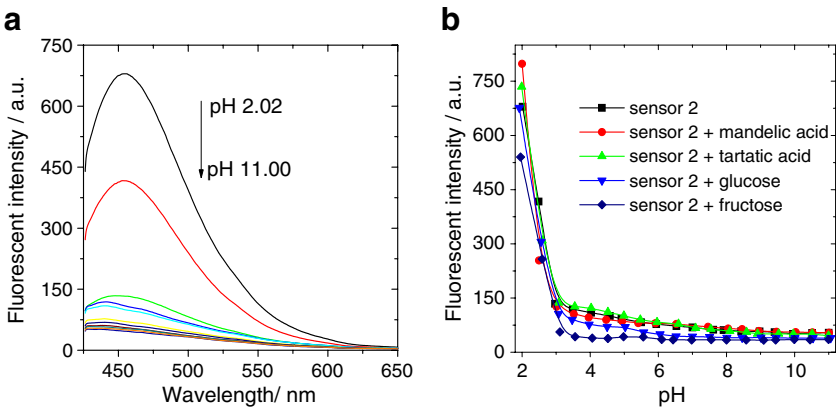


**Fig. 4** Fluorescent intensity-pH profile of sensor **2**. (**a**) the emission spectral changes vs. pH of the solution. (**b**) the pH titration curves of the sensor **2** in the presence of various analytes (0.025 mol $dm^{-3}$). λex =400 nm, λem=412 nm. $5.0\times10^{-6}$ mol $dm^{-3}$ of sensor 2 in 0.05 mol $dm^{-3}$ NaCl ionic buffer (52.1% methanol in water). 20°C

sensor **1** is more sensitive to the polarity of the solvents than sensor **2**. For example, with switch the solvent from hexane to methanol, the emission of sensor **1** red-shifted by 31 nm (from 389 nm to 420 nm). For sensor **2**, however, the emission red-shifted by only 13 nm (from 393 nm to 406 nm). Furthermore, the results show that the emission of sensor **1** in methanol is comparable to that in acetonitrile ($I_{MeOH}/I_{MeCN} = 1.43$). For sensor **2**, however, the emission in MeOH is much weaker than that in MeCN ($I_{MeOH}/I_{MeCN} = 0.37$). The solvent polarity of MeOH and MeCN is similar, thus the more significant quenching effect of MeOH on the emission of sensor **2** is most probably due to the solute-solvent hydrogen bonding. With the MeOH/$H_2O$ buffer used, the emission of sensor **1** is diminished but the emission of sensor **2** was completely quenched (Fig. 5). Thus the weak emission of sensor **2** in protic solvents is due to the quenching effect of the solute-solvent H-bonding.

Inspired by the recent applications of DFT /TDDFT calculations in chemosensor research [42, 43, 45–49], we carried out DFT/TDDFT calculations on the photophysical properties of the sensors **1** and **2** prior to their synthesis. d-PET effect was predicted for sensor **1** and sensor **2** (Fig. 6 and Table 1).

The molecular orbitals involved in the low-lying electronic transitions of sensor **1** and **2** are summarized in Fig. 6 and Table 1. It was found the lowest-lying excited state ($S_1$) of the protonated sensor **1** is characterized with small oscillator strength (*f*), for example, the f values of protonated sensor 1 is 0.0892. Inspection of the MOs involved in this transition show that there is no overlap between the HOMO and the LUMO orbital (Fig. 6). Thus, we concluded that the transition $S_1 \leftarrow S_0$ is basically a forbidden transition and $S_1$ state of the protonated sensor **1** is dark state, i.e. the protonated sensor **1** should show weak emission [45, 46, 54]. For the neutral sensor **1**, however, much higher oscillator strength was found for the $S_1$ state. Correspondingly overlap was found for the MOs.

Thus the $S_1$ state of the neutral sensor **1** is an allowed transition, infers that neutral sensor **1** is probably strongly fluorescent. Same calculation results were obtained for sensor **2** (see Supplementary data). These calculations predicted d-PET effect for sensor **1** and sensor **2**, i.e. the sensors will show diminished fluorescence in the acidic pH range, but enhanced emission intensity at neutral and basic pH [42, 43, 55]. This kind of fluorescence transduction is in contrast to the widely reported a-PET sensors [1–3]. The calculated UV-Vis absorption of sensor **1** and sensor **2** are in good agreement with the experimental observations. For example, the predicted absorption wavelength 403 nm of sensor **1** is close to the experimental observation of 392 nm

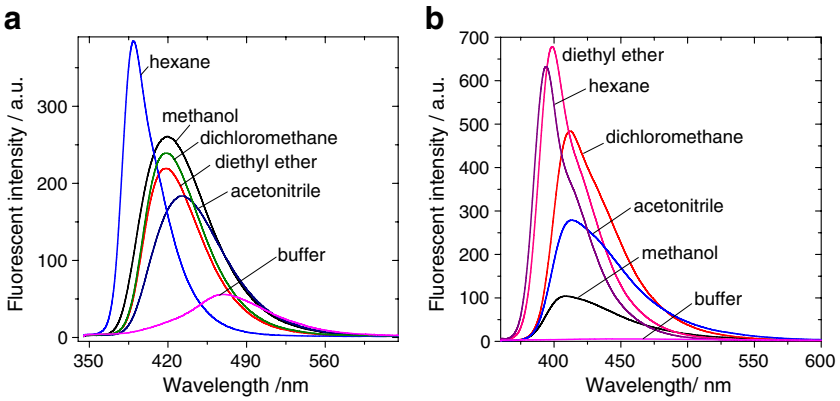


**Fig. 5** Emission spectra of (**a**) sensor **1**, λex=375 nm and (**b**) sensor **2**, λex=350 nm in different solvents. $1.0\times10^{-6}$ mol $dm^{-3}$ of sensors in different solvents. Buffer: 0.05 mol $dm^{-3}$ NaCl ionic buffer (52.1% methanol in water). pH 7.0. 20°C

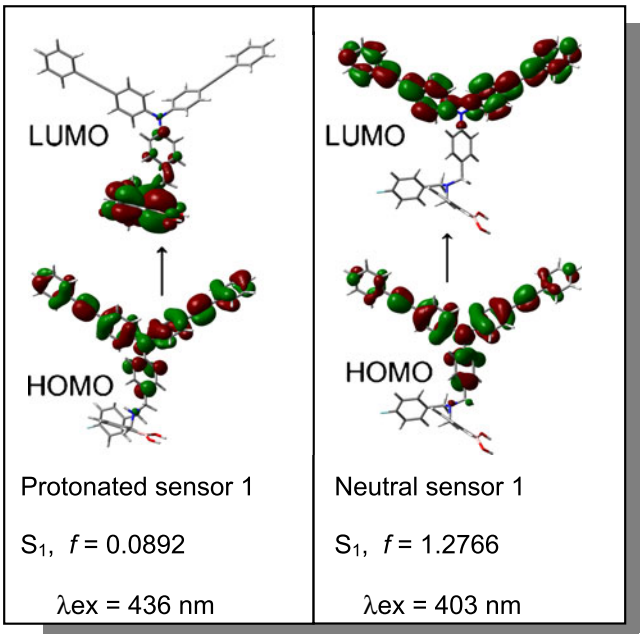


**Fig. 6** Prediction of the d-PET effect for sensor **1** by DFT/TDDFT calculations. (**a**) The main transitions of the singlet excited state of the protonated sensor **1**. $S_1 \leftarrow S_0$ (LUMO←HOMO). Note $S_1$ is a dark state with no overlap between the HOMO and LUMO MOs and the oscillator strength $f$=0.0892, featured with ICT character. (**b**) The main transitions of the singlet excited state of the neutral sensor **1**, $S_1 \leftarrow S_0$ (LUMO ← HOMO). Note $S_1 \leftarrow S_0$ of neutral sensor **1** is an allowed electronic transition with oscillator strength $f$=1.2766 and basically recognized as a LE state

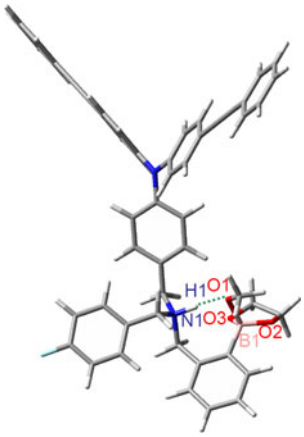


**Fig. 7** View of the binding complex of sensor **1** with ethylene glycol showing the zwitterionic structure with intramolecular hydrogen binding. A MeOH molecular is inserted in the B-N interaction. The *dotted line* is indicative of the H-bonding interaction with geometry: N1-H1···O1, N···O 2.649 Å, H···O 1.572 Å, N-H 1.082 Å , N-H···O 173°

(Fig. 1). For sensor **2**, the calculated excitation energy is 409 nm, which is in good agreement with the observed 412 nm (see Supplementary Material).

The DFT/TDDFT calculations predict d-PET effect for both sensor **1** and sensor **2**. However, a-PET effect was observed for sensor **1** and no significant PET effect was observed for sensor **2** (Fig. 2 and Fig. 4). The discrepancy between the theoretical predictions and the experimental observations inspired us to rationalize the photophysics of the sensors from a different point of view.

For sensor **2**, no significant PET effect was observed, we envision that the energy level of the HOMO orbital of this molecule maybe higher than the energy level of the lone pair electron of the nitrogen atom, thus the fluorescence

**Table 1** Selected electronic excitation energies (eV) and corresponding oscillator strengths (*f*), main configurations and CI coefficients of the low-lying electronically excited states of the protonated sensor **1** ($[1\text{-H}]^+$) and neutral sensor **1**. Calculated by TDDFT//B3LYP/6-31G(d), Based on the DFT//B3LYP/6-31G(d) optimized ground state geometries

| Sensor | Electronic transitions | TDDFT//B3LYP/6-31G(d) | | | |
|---|---|---|---|---|---|
| | | Energy[a] /eV(nm) | *f*[b] | Composition[c] | CI[d] |
| $[1+H]^+$ | $S_0 \rightarrow S_1$ | 2.84 (436) | 0.0892 | H→L | 0.7000 |
| | $S_0 \rightarrow S_2$ | 3.14 (394) | 0.1536 | H-1→L+1 | 0.6072 |
| | $S_0 \rightarrow S_3$ | 3.25 (381) | 0.1513 | H→L+2 | 0.1513 |
| | $S_0 \rightarrow S_5$ | 3.37 (368) | 0.8526 | H→L+4 | 0.5710 |
| | | | | H→L+3 | 0.2966 |
| 1 | $S_0 \rightarrow S_1$ | 3.08 (403) | 1.2766 | H→L | 0.6713 |
| | $S_0 \rightarrow S_2$ | 3.40 (365) | 0.4735 | H→L+1 | 0.6656 |
| | $S_0 \rightarrow S_3$ | 0.78 (330) | 0.4735 | H→L+2 | 0.1454 |
| | | | 0.6630 | H→L+3 | 0.6630 |
| | $S_0 \rightarrow S_4$ | 3.99 (310) | 0.2122 | H-1→L | 0.3972 |
| | | | | H→L+2 | 0.5078 |
| | | | | H→L+4 | 0.2315 |

[a] Only the low-lying excited states and some allowed transitions were presented

[b] Oscillator strength

[c] Only the main configurations are presented. H stands for HOMO and L stands for LUMO

[d] The CI coefficients are in absolute values

emission of the fluorophore cannot be modulated by the N atom [30, 44]. The DFT calculation shows the HOMO energy level of sensor **2** (−3.59 eV) is significantly increased compared to sensor **1** (with HOMO energy level of −4.82 eV). Thus we propose the high HOMO energy level of sensor **2** is responsible for its lack of PET effect [30].

It was known that the PET effect of boronic acid sensors is modulated by the B-N interaction, which can be strengthened upon binding analyte molecules, thus the PET (with N as the electron donor and the fluorophore as the electron acceptor) was suppressed and as a result, the fluorescence emission intensity was enhanced [1–3, 30]. However, single crystal structures demonstrated that a solvent inserted structured formed for the complex, at least in protic solvents [6, 9, 32]. We used DFT methods to study the proposed intramolecular hydrogen bond of the binding complex (Fig. 7).

The optimized structure is zwitterionic form, which is in agreement with the single crystal structures of the boronic acid-analyte binding complexes. The hydrogen bond length is (N-H····O) 2.649 Å, which is close to the reported value of 2.64–2.73 Å for the boronate complexes [9, 16, 32]. The optimized O····B distance is 1.546 Å, also close to the reported 1.477 Å [9, 32]. These results demonstrate that the binding complex of the boronic acid sensor can be studied with the DFT calculations. To our knowledge, this is first time the structure of the bonded boronic acid sensor with solvent-inserted, zwitterionic structure with intramolecular hydrogen bonding was studied with the DFT optimization method.

In summary, new ethynylated triphenylamine boronic acid sensor **1** and **2** were designed and the photophysical properties, as well as the binding with tartaric acid and mandelic acid were studied. DFT/TDDFT calculations on the low-lying excited states of these sensors predicted d-PET effect. But experimental observations show a-PET effect for sensor **1** and no significant PET effect was found for sensor **2**. The discrepancy between the theoretical prediction and the experimental results can be rationalized by considering the energy levels of the HOMO of sensors **2**. The much higher energy level of the HOMO orbital of sensor **2** (−3.59 eV) than sensor **1** (−4.82 eV) infer that the *N* atom cannot modulate the fluorescence, thus eliminate the PET effect of sensor **2**. Our results demonstrated the promising applications of DFT/TDDFT calculation on prediction the photophysical properties of the fluorescent sensors. These systematic studies on the photophysics of the fluorescent sensors and the application of theoretical calculation in the study of the fluorescent sensors are of great interest for development of new fluorescent sensors and fluorophores with predetermined photophysical properties.

**Acknowledgements** We thank the NSFC (20642003, 40806042, 20634040 and 20972024), Ministry of Education (SRF for ROCS, SRFDP-200801410004 and NCET-08-0077), PCSIRT (IRT0711), State Key Laboratory of Fine Chemicals (KF0710 and KF0802), State Key Laboratory of Chemo/Biosensing and Chemometrics (2008009), the Education Department of Liaoning Province (2009 T015) and Dalian University of Technology (SFDUT07005 and 1000-893394) for financial support. We are grateful to RS (UK) and NSFC (China) for the Cost-Share program and the annual CASE symposium.

## References

1. James TD (2007) Saccharide-selective boronic acid based Photo-induced Electron Transfer (PET) fluorescent sensors. Top Curr Chem 277:107–152
2. Fujita N, Shinkai S, James TD (2008) Boronic acids in molecular self-assembly. Chem Asian J 3:1076–1091
3. James TD, Shinkai S (2002) Artificial receptors as chemosensors for carbohydrates. Top Curr Chem 218:159–200
4. Zhu L, Shabbir SH, Gray M, Lynch VM, Sorey S, Anslyn EV (2006) A structural investigation of the N-B interaction in an o-(N, N-Dialkylaminomethyl)arylboronate system. J Am Chem Soc 128:1222–1232
5. Tan W, Zhang D, Wang Z, Liu C, Zhu D (2007) 4-(N, N-Dimethylamine)benzonitrile (DMABN) derivatives with boronic acid and boronate groups: new fluorescent sensors for saccharides and fluoride ion. J Mater Chem 17:1964–1968
6. Jin S, Li M, Zhu C, Tran V, Wang B (2008) Computer-based de novo design, synthesis, and evaluation of boronic acid-based artificial receptors for selective recognition of dopamine. ChemBioChem 9:1431–1438
7. Wang J, Jin S, Akol S, Wang B (2007) Design and synthesis of long-wavelength fluorescent boronic acid reporter compounds. Eur J Org Chem 2091–2099.
8. DiCesare N, Adhikari DP, Heynekamp JJ, Heagy MD, Lakowicz JR (2002) Spectroscopic and photophysical characterization of fluorescent chemosensors for monosaccharides based on N-Phenylboronic acid derivatives of 1, 8-Naphthalimide. J Fluoresc 12:147–154
9. Zhang L, Kerszulis JA, Clark RJ, Ye T, Zhu L (2009) Catechol boronate formation and its electrochemical oxidation. Chem Commun (16):2151–2153
10. Trupp S, Schweitzer A, Mohr GJ (2006) A fluorescent water-soluble naphthalimide-based receptor for saccharides with highest sensitivity in the physiological pH range. Org Biomol Chem 4:2965–2968
11. Wang Z, Zhang D, Zhu D (2005) A new saccharide sensor based on a tetrathiafulvalene anthracene dyad with a boronic acid group. J Org Chem 70:5729–5732
12. Sun X-Y, Liu B (2005) The fluorescence sensor for saccharide based on internal conversion. Luminescence 20:331–333
13. Xu W, Huang Z, Zheng Q (2008) Highly efficient fluorescent sensing for a-hydroxy acids with C3-symmetric boronic acid-based receptors. Tetrahedron Lett 49:4918–4921
14. Davis CJ, Lewis PT, Billodeaux DR, Fronczek FR, Escobedo JO, Strongin RM (2001) Solid-state supramolecular structures of resorcinol—arylboronic acid compounds. Org Lett 3:2443–2445
15. Manimala JC, Wiskur SL, Ellington AD, Anslyn EV (2004) Tuning the specificity of a synthetic receptor using a selected nucleic acid receptor. J Am Chem Soc 126:16515–16519
16. Collins BE, Sorey S, Hargrove AE, Shabbir SH, Lynch VM, Anslyn EV (2009) Probing intramolecular B-N interactions in ortho-aminomethyl arylboronic acids. J Org Chem 74:4055–4060

17. Gamsey S, Miller A, Olmstead MM, Beavers CM, Hirayama LC, Pradhan S, Wessling RA, Singaram B (2007) Boronic acid-based bipyridinium salts as tunable receptors for monosaccharides and —hydroxycarboxylates. J Am Chem Soc 129:1278–1286
18. Kawanishi T, Romey MA, Zhu P, Holody MZ, Shinkai S (2004) A study of boronic acid based fluorescent glucose sensors. J Fluoresc 14:499–512
19. Cappuccio FE, Suri JT, Cordes DB, Wessling RA, Singaram B (2004) Evaluation of pyranine derivatives in boronic acid based saccharide sensing: Significance of charge interaction between dye and quencher in solution and hydrogel. J Fluoresc 14:521–533
20. Pu L (2004) Fluorescence of organic molecules in chiral recognition. Chem Rev 104:1687–1716
21. Qin H, He Y, Hu C, Chen Z, Hu L (2007) Enantioselective fluorescent sensor for dibenzoyl tartrate anion based on chiral binaphthyl derivatives bearing an amino acid unit. Tetrahedron Asymmetr 18:1769–1774
22. Zhu K, Zhang M, Wang F, Li N, Li S, Huang F (2008) Improved complexation between dibenzo-24-crown-8 derivatives and dibenzylammonium salts by ion-pair recognition. New J Chem 32:1827–1830
23. He C, Shi Z, Zhou Q, Li S, Li N, Huang F (2008) Syntheses of cis- and trans-Dibenzo-30-Crown-10 derivatives via regioselective routes and their complexations with paraquat and diquat. J Org Chem 73:5872–5880
24. Xu X-N, Wang L, Wang G-T, Lin J-B, Li G-B, Jiang X-K, Li Z-T (2009) Hydrogen-bonding-mediated dynamic covalent synthesis of macrocycles and capsules: new receptors for aliphatic ammonium ions and the Formation of Pseudo[3]rotaxanes. Chem Eur J 15:5763–5774
25. Wickramasinghe Y, Yang Y, Spencer SA (2004) Current problems and potential techniques in in vivo glucose monitoring. J Fluoresc 14:513–520
26. Moschou EA, Sharma BV, Deo SK, Daunert S (2004) Fluorescence glucose detection: advances toward the ideal in vivo biosensor. J Fluoresc 14:535–547
27. Schäferling M, Wu M, Wolfbeis OS (2004) Time-resolved fluorescent imaging of glucose. J Fluoresc 14:561–568
28. Badugu R, Lakowicz JR, Geddes CD (2004) Ophthalmic glucose monitoring using disposable contact lenses—a review. J Fluoresc 14:617–613
29. Yang XP, Lee MC, Sartain F, Pan XH, Lowe CR (2006) Designed boronate ligands for glucose-selective holographic sensors. Chem Eur J 12:8491–8497
30. De Silva AP, Gunaratne HQN, Gunnlaugsson T, Huxley AJM, McCoy CP, Rademacher JT, Rice TE (1997) Signaling recognition events with fluorescent sensors and switches. Chem Rev 97:1515–1566
31. James TD, Samankumara Sandanayake KRA, Iguchi R, Shinkai S (1995) Novel saccharide-photoinduced electron transfer sensors based on the interaction of boronic acid and amine. J Am Chem Soc 117:8982–8987
32. Zhao J, Davidson MG, Mahon MF, Kociok-Kohn G, James TD (2004) An enantioselective fluorescent sensor for sugar acids. J Am Chem Soc 126:16179–16186
33. Zhao J, James TD (2005) An enantioselective fluorescent sensor for sugar acids. J Mater Chem 15:2896–2901
34. Chi L, Zhao J, James TD (2008) Chiral mono boronic acid as fluorescent enantioselective sensor for Mono$\alpha$-hydroxyl carboxylic acids. J Org Chem 73:4684–4687
35. Cao HS, Diaz DI, DiCesare N, Lakowicz JR, Heagy MD (2002) Monoboronic acid sensor that displays anomalous fluorescence sensitivity to glucose. Org Lett 4:1503–1505
36. Jin S, Wang J, Li M, Wang B (2008) Synthesis, evaluation, and computational studies of naphthalimide-based long-wavelength fluorescent boronic acid reporters. Chem Eur J 14:2795–2804
37. James TD, Shinmori H, Shinkai S (1997) Novel fluorescence sensor for 'small' saccharides. Chem Commun 71
38. Gao X, Zhang Y, Wang B (2003) New boronic acid fluorescent reporter compounds. 2. A naphthalene-based on — off sensor functional at physiological pH. Org Lett 5:4616–4618
39. Zhao J, Fyles TM, James TD (2004) Chiral Binol—Bisboronic acid as fluorescence sensor for sugar acids. Angew Chem Int Ed 43:3461–3464
40. Zhao J, James TD (2005) Enhanced fluorescence and chiral discrimination for tartaric acid in a dual fluorophore boronic acid receptor. Chem Commun 1889–1891.
41. Liang X, James TD, Zhao J (2008) 6, 6′-Bis-substituted BINOL boronic acids as enantioselective and chemselective fluorescent chemosensors for D-sorbitol. Tetrahedron 64:1309–1315
42. Han F, Chi L, Liang X, Ji S, Liu S, Zhou F, Wu Y, Han K, Zhao J, James TD (2009) 3, 6-Disubstituted Carbazole-Based bisboronic acids with unusual fluorescence transduction as enantioselective fluorescent chemosensors for tartaric acid. J Org Chem 74:1333–1336
43. Zhang X, Chi L, Ji S, Wu Y, Song P, Han K, Guo H, James TD, Zhao J (2009) Rational design of d-PeT Phenylethynylated-Carbazole monoboronic acid fluorescent sensors for the selective detection of $\alpha$-Hydroxyl carboxylic acids and monosaccharides. J Am Chem Soc 131:17452–17463
44. Valeur B (2001) Molecular fluorescence: principles and applications. Wiley—VCH Verlag GmbH, New York
45. Ji S, Yang J, Yang Q, Liu S, Chen M, Zhao J (2009) Tuning the intramolecular charge transfer of alkynylpyrenes: effection photophysical properties and its application in design of OFF-ON fluorescent thiol probes. J Org Chem 74:4855–4865
46. Zhao G-J, Liu J-Y, Zhou J-C, Han K-L (2007) Site-selective photoinduced electron transfer from alcoholic solvents to the chromophore facilitated by hydrogen bonding: a new fluorescence quenching mechanism. J Phys Chem B 111:8940–8945
47. Liu Y, Feng J, Ren A (2008) Theoretical study on photophysical properties of Bis-Dipolar Diphenylamino-endcapped oligoarylfluorenes as light-emitting materials. J Phys Chem A 112:3157–3164
48. Li M-X, Zhang H-X, Zhou X, Pan Q-J, Fu H-G, Sun C-C (2007) Theoretical studies of the electronic structure and spectroscopic properties of $[Ru(Htcterpy)(NCS)_3]^{3-}$. Eur J Inorg Chem 2171–2180
49. Li M-X, Zhou X, Xia B-H, Zhang H-X, Pan Q-J, Liu T, Fu H-G, Sun C-C (2008) Theoretical studies on structures and spectroscopic properties of photoelectrochemical cell ruthenium sensitizers, $[Ru(Hmtcterpy)(NCS)_3]^{n-}$ (m=0, 1, 2, and 3; n=4, 3, 2, and 1). Inorg Chem 47:2312–2324
50. Frisch MJ, Trucks GW, Schlegel HB, Scuseria GE, Robb MA, Cheeseman JR, Montgomery JA Jr, Vreven T, Kudin KN, Burant JC, Millam JM, Iyengar SS, Tomasi J, Barone V, Mennucci B, Cossi M, Scalmani G, Rega N, Petersson GA, Nakatsuji H, Hada M, Ehara M, Toyota K, Fukuda R, Hasegawa J, Ishida M, Nakajima T, Honda Y, Kitao O, Nakai H, Klene M, Li X, Knox JE, Hratchian HP, Cross JB, Bakken V, Adamo C, Jaramillo J, Gomperts R, Stratmann RE, Yazyev O, Austin AJ, Cammi R, Pomelli C, Ochterski JW, Ayala PY, Morokuma K, Voth GA, Salvador P, Dannenberg JJ, Zakrzewski VG, Dapprich S, Daniels AD, Strain MC, Farkas O, Malick DK, Rabuck AD, Raghavachari K, Foresman JB, Ortiz JV, Cui Q, Baboul AG, Clifford S, Cioslowski J, Stefanov BB, Liu G, Liashenko A, Piskorz P, Komaromi I, Martin RL, Fox DJ, Keith T, Al-Laham MA, Peng CY, Nanayakkara A, Challacombe M, Gill PMW, Johnson B, Chen W, Wong MW, Gonzalez C, Pople JA (2004) Gaussian 03 Revision D.01. Gaussian Inc., Wallingford
51. Ueno T, Urano Y, Setsukinai K, Takakusa H, Kojima H, Kikuchi K, Ohkubo K, Fukuzumi S, Nagano T (2004) Rational principles

for modulating fluorescence properties of fluorescein. J Am Chem Soc 126:14079–14085
52. Tucker SH (1926) Iodination in the carbaxole series. J Chem Soc 546–553
53. Zhao G, Chen R, Sun M, Liu J, Li G, Gao Y, Han K, Yang X, Sun L (2008) Photoinduced intramolecular charge transfer and $S_2$ fluorescence in Thiophene-π-conjugated donor—acceptor systems: experimental and TDDFT studies. Chem Eur J 14:6935–6947
54. Han F, Chi L, Wu W, Liang X, Fu M, Zhao J (2008) Environment sensitive phenothiazine dyes strongly fluorescence in protic solvents. J Photochem Photobiol A Chem 196:10–23
55. Sunahara H, Urano Y, Kojima H, Nagano T (2007) Design and synthesis of a library of BODIPY-Based environmental polarity sensors utilizing photoinduced electron-transfer-controlled fluorescence ON/OFF switching. J Am Chem Soc 129:5597–5604